18th Australasian Fluid Mechanics Conference
Launceston, Australia
3-7 December 2012

Suppression of the Trailing-Edge Noise Using a Plasma Actuator

A. Inasawa[1], C. Ninomiya[1] and M. Asai[1]

[1]Department of Aerospace Engineering, Tokyo Metropolitan University

6-6 Asahigaoka, Hino, Tokyo 191-0065, JAPAN

Abstract

Suppression control of noise generation at an airfoil trailing edge was conducted using a plasma actuator for a NACA0012 airfoil with an angle of attack of 2° at a chord Reynolds number $Re = 2.2 \times 10^5$ where generation of tonal trailing-edge noise was governed by vortex roll-up of boundary layer on the pressure surface in the vicinity of the trailing-edge. To minimize possible interferences of electrode installation to the boundary-layer stability, a specially-designed actuator with flush-mounted configuration was employed. It was found that when the actuator was installed at 55%-60% chord location on the pressure surface, a weak surface flow induced by the actuator stabilized the boundary layer significantly to suppress the strong growth of instability waves, which is responsible for the occurrence of the acoustic feedback. As a result, the complete suppression of the trailing-edge noise could be achieved successfully.

Introduction

The methodology of effective flow control leading to the reduction of aerodynamic sound is one of the key technologies in developing next generation aircraft. Among the flow control techniques developed thus far, the plasma actuator (PA) [2] is of particular interest as one of the new flow control devices, and its ability of flow control has been demonstrated in several flows such as the boundary-layer separation on the airfoils [9], and vortex shedding in the bluff body wake [12]. In the present flow control experiment using PA, we focus on the suppression of the trailing-edge noise of an airfoil.

Regarding airfoil trailing-edge noise, a number of experimental and numerical studies have been conducted to understand the mechanism of tonal noise generation at the trailing edge since the pioneering experiment by Paterson et al. [8]. Arbey and Bataille [1] examined the mechanism of discrete tones observed by Paterson et al. and proposed a feedback-loop model between the boundary-layer instability waves (the growth of Tollmien-Schlichting) and the acoustic waves. The feedback-loop mechanism was supported by recent experimental [7,5] and numerical [3] results. Therefore, we may expect that if the development of instability waves (i.e., Tollmien-Schlichting waves in the airfoil boundary layer) is sufficiently suppressed, the acoustic feedback-loop mechanism leading to the trailing-edge noise generation does not work. Here, one should pay close attention to the configuration of actuator in controlling boundary layer stability because the boundary-layer transition is strongly affected by slight changes in the wall geometry [6,10,11,4]. Most of the previous flow control experiments using PA, the exposed electrode was located on the wall surface, forming a step like isolated roughness. Such projection from the wall surface is necessary to induce strong surface flow though it acts as an isolated roughness element which may promote boundary-layer transition, especially when the boundary layer thickness becomes thinner as freestream velocity is increased.

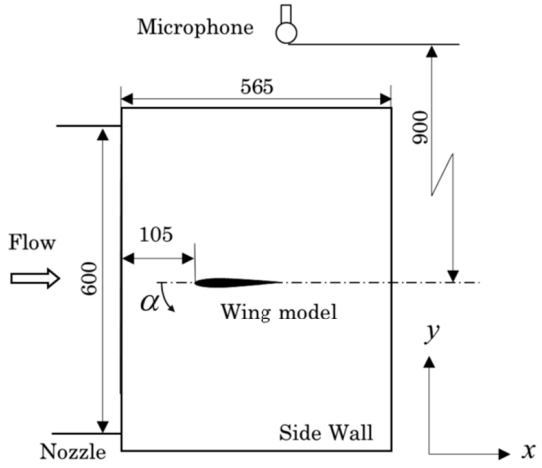

Figure 1. Experimental setup (dimensions in mm).

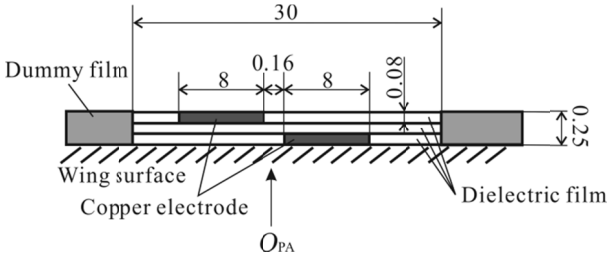

Figure 2. Schematics of the plasma actuator with flush-mounted electrode configuration (dimensions in mm).

In the present study, a plasma actuator with flush-mounted electrode configuration was employed to minimize possible interferences of actuator installation to the boundary layer transition, and its ability to stabilize the boundary layer and suppress the trailing-edge noise was examined experimentally.

Experimental setup and procedure

The experiment was conducted in an open-jet type wind tunnel with an exit cross-section of 600 mm (height) × 300 mm (span). The turbulence intensity at the tunnel exit was less than 0.1 % of the free-stream velocity in terms of the root mean square (r.m.s.) value of the streamwise velocity fluctuation. Two Plexiglas sidewalls maintained the two-dimensionality of the main stream in the test section although the upper and lower areas were opened. A NACA0012 wing model made of aluminum whose chord (c) and span (s) were 150 mm and 298 mm, respectively, was set between the side walls (Fig. 1). To measure the trailing-

edge noise, a microphone was installed 900 mm above the wing trailing-edge. The coordinates x and y represent streamwise and vertical directions, respectively, measured from the spanwise (z) center of the wing leading-edge. The angle of attack was measured toward the pitch down direction.

For flow control, a plasma actuator of Single Dielectric-Barrier-Discharge (SDBD) type was used. The PA consisted of copper electrodes and polyimid (Kapton) film. To minimize the possible interference of electrode installation in the boundary-layer stability, a specially-designed actuator with flush-mounted electrode configuration was employed (Fig. 2). The chordwise location of the actuator installation (the center of the actuator, O_{PA}) is denoted by x_{PA}. The actuator spans a lateral distance s_{PA}=270mm. To maintain the smoothness of the wing surface, the wing surface (other than the actuator) was covered with a 250μm-thick polyvinyl choroid film. The actuator was driven with a continuous sinusoidal signal of 15kHz which was amplified by an audio power amplifier and boosted in voltage by a transformer. The flow control was accomplished with an input voltage of E_{PA}=3kV. A particle image velocimetry (PIV) system (Dantec) consisting of a double-pulsed Nd:Yag laser and a CCD camera of 1280 × 1024 pixels was used to obtain instantaneous velocity and vorticity fields. A laser Doppler velocimetry (LDV) system (Dantec) was also used to examine the blowing effect of the actuator in detail. The velocity of the oncoming uniform flow was fixed at U_∞=21m/s and the chord-Reynolds number was 2.2 × 10^5. The angle of attack α was fixed at 2°.

Results and discussion

Figure 3 illustrates the power spectra of the sound pressure level (SPL) with and without the wing model in the test section at α= 2° at U_∞=21m/s (Re=2.2 × 10^5). Here, the plasma actuator is not installed on the wing surface. We see a distinct discrete tone with the frequency of f_T = 998Hz whose magnitude is 40dB larger in the presence of the wing than the background noise level. Figures 4(a) and 4(b) illustrate instantaneous vorticity and cross-stream velocity near the trailing edge, respectively. Here, the double-frame PIV images were captured and synchronized with the signal of the trailing-edge noise measured by the microphone. One of 150 snapshots is displayed in the figure. We see the development of periodic vortices immediately upstream of the trailing edge on pressure (upper) surface (Fig. 4a), indicating that the instability waves (Tollmien-Schlichting waves) of the selected discrete (or narrow-band) frequency were excited in the pressure-side boundary-layer by the acoustic feedback mechanism. These vortices can produce a strong pressure fluctuation i.e., the trailing-edge acoustic dipole by diffraction of vortex-induced cross-stream fluctuation at the trailing-edge, as shown in Fig. 4(b). On the suction (lower) surface, on the other hand, the boundary layer had already undergone transition to turbulence far upstream of the trailing edge so that periodic vortex formation little appeared around the trailing edge. Then, we next applied flow control on the pressure-side boundary-layer.

Figure 5 illustrates the effect of noise suppression by the actuator at chordwise locations of x_{PA}/c=0.55. We see that the installation of the present actuator with flush-mounted electrode configuration only had a minor effect on the boundary-layer instability as understood from the fact that the frequency and sound pressure level (SPL) did not change compared with those in the natural sound radiation (see Fig. 3). The sound pressure level of the trailing-edge noise at f=f_T, SPL_T, decreased down to the background noise level when the actuator was operated at x_{PA}/c=0.55 (Fig. 5). Figure 6 illustrates the dependency of the

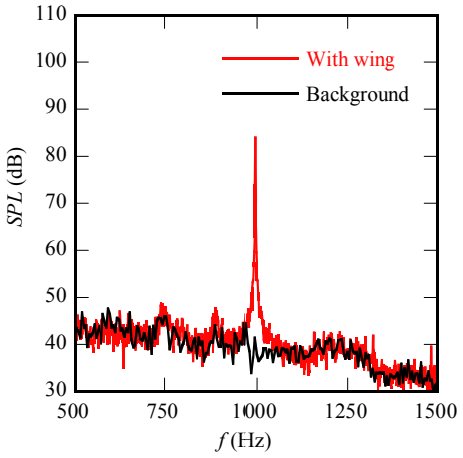

Figure 3. The SPL of radiated sound from a single NACA0012 airfoil (α=2° , U_∞=21m/s, Re=2.2×10^5).

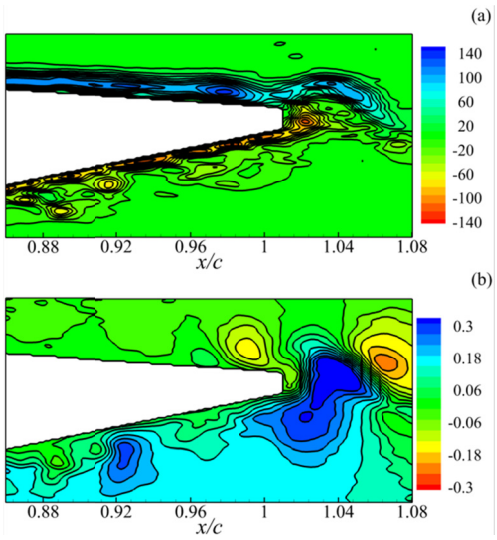

Figure 4. Instantaneous (a) vorticity $\omega c/U_\infty$ and (b) cross-stream velocity fluctuation v/U_∞ near the trailing-edge without actuator installation (α=2°).

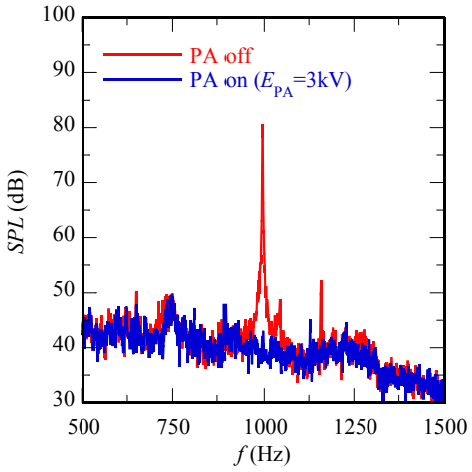

Figure 5. SPL vs. frequency with and without actuator operation at x_{PA}/c=0.55.

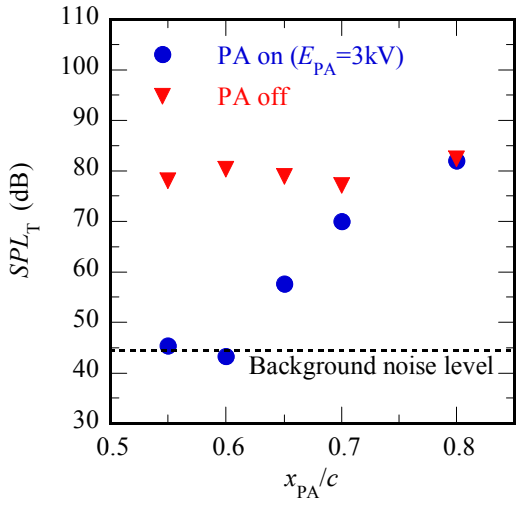

Figure 6. Chordwise variation of SPL of the trailing-edge noise at α=2°.

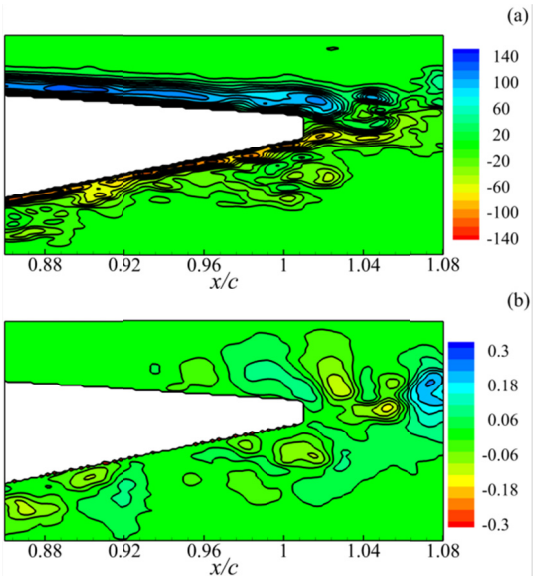

Figure 7. Instantaneous (a) vorticity $\omega c/U_\infty$ and (b) cross-stream velocity fluctuation v/U_∞ near the trailing-edge with actuator operation at x_{PA}/c=0.55 (E_{PA}=3kV).

noise reduction on the actuator location (x_{PA}/c), showing that the SPL of the trailing-edge noise decreased rapidly as the actuator location moved upstream and could be suppressed completely when the actuator was set near x_{PA}/c = 0.6, indicating that the suppression control of the trailing-edge noise can be achieved most effectively when the actuator is operated at and around x_{PA}/c=0.55-0.6 at this angle of attack. Here it is important to mention that the adverse pressure gradient begins around x/c=0.25 and increases appreciably beyond x/c=0.6 on the pressure side at a 2° angle of attack for the NACA0012 airfoil. Figures 7(a) and 7(b) demonstrate the instantaneous vorticity and cross-stream velocity fields, respectively, for the plasma actuator operated at x_{PA}/c=0.55. No vortex roll-up was found on the pressure (upper) side, while the turbulent boundary-layer still developed on the suction (lower) side (Fig. 7a). In addition, the diffraction of the cross-flow velocity fluctuation at the trailing edge became weak (Fig. 7b). Thus, it is understood that the trailing-edge noise is suppressed completely by inhibiting the development of instability waves into strong vortices near the

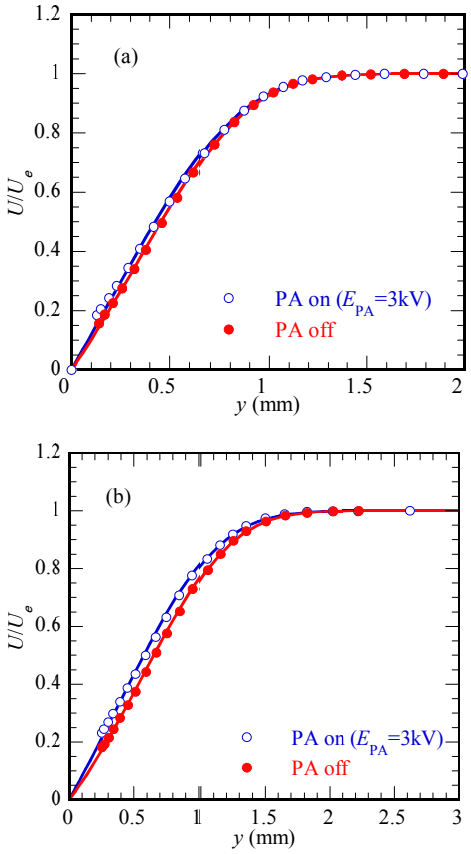

Figure 8. The y-distribution of mean velocity at (a) x/c=0.6 and (b) x/c=0.9 (x_{PA}/c=0.55). The solid lines represent the Falkner-Skan boundary layer profile.

trailing edge. Then, we examined the near-wall flow developing downstream of the actuator in detail by means of laser Doppler velocimetry (LDV). Figures 8(a) compares the normal-to-wall (y) distribution of time-averaged streamwise velocity U at x/c=0.6, immediately downstream of the actuator installed at x_{PA}/c =0.55, with and without the plasma actuator operation. We observed a slight increase in the streamwise velocity U inside the boundary layer ($y \lesssim$ 1mm). The velocity excess by the actuator operation was at most about 4% of the uniform flow velocity, i.e., 0.84m/s, showing that the blowing flow was induced close to the wall despite the flush-mounted electrode configuration. Such weak surface flow, however, could markedly alter the boundary-layer velocity profiles at the downstream locations up to the trailing edge as shown in Fig. 8(b), which compares the velocity profiles at x/c=0.9 with and without the actuator operation. The boundary-layer profile under the actuator operation is not inflectional near the trailing edge (Fig. 8b). To investigate the noise suppression from the instability viewpoint, we conducted the linear stability analysis for the velocity distributions shown in Figs. 8(a) and 8(b). The Falkner-Skan velocity profile was used to model the boundary layer profiles under non-zero pressure gradients on the pressure surface. The approximated velocity profiles are shown by the solid and broken lines in Figs. 8(a) and 8(b). The linear stability of these velocity profiles was analysed by solving the Orr-Sommerfeld equation. The spatial growth rates calculated for the approximated profiles at x/c=0.6 and 0.9 are plotted in Fig. 9, in which the frequency of trailing-edge noise (998Hz) is drawn by the broken curves. In the case of no actuator operation, we see that the unstable frequency range both at x/c=0.6 and x/c=0.9 includes the frequency of the trailing- edge noise. When the

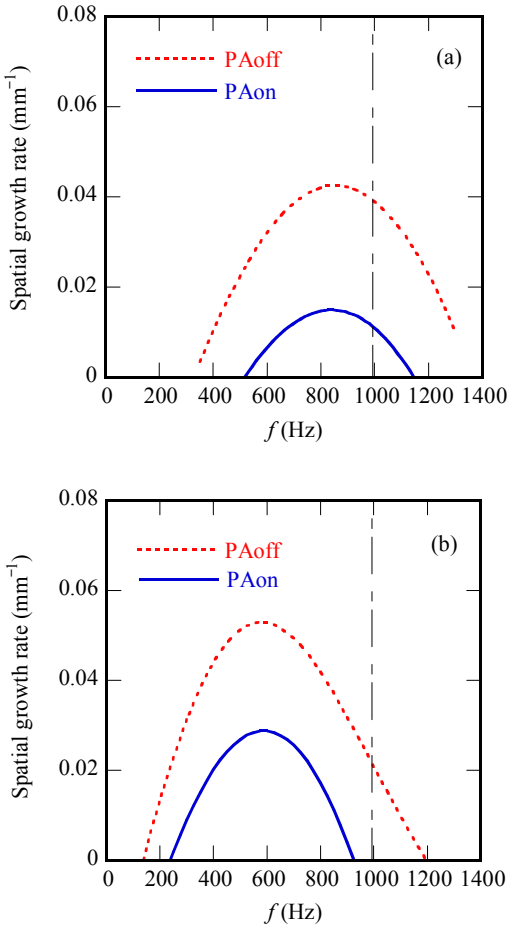

Figure 9. The spatial growth rate of linear disturbances predicted by the Orr-Sommerfeld equation (x_{PA}/c=0.55). (a) x/c=0.6 and (b) x/c=0.9. Chain lines represent the frequency of the trailing-edge noise.

actuator was operated, on the other hand, the growth rate decreased drastically down to about one-third of that without actuator operation at x/c=0.6, and the linear disturbance at tonal noise frequency became stable at x/c=0.9.

Conclusion

Suppression control of noise generation at an airfoil trailing edge was conducted by using a plasma actuator for a NACA0012 airfoil at an angle of attack of 2°, at a chord Reynolds number $Re = 2.2\times10^5$, where the generation of tonal trailing-edge noise was governed by the acoustic feedback loop mechanism operating on the pressure surface. To minimize possible interferences of electrode installation to the boundary-layer stability, we used an actuator with a flush-mounted electrode configuration. The effective suppression of the trailing-edge noise was achieved when the plasma actuator was operated at 55%-60% chord location. In this effective condition, the magnitude of actuator induced near wall flow velocity was at most 4% of the uniform flow velocity. It was also demonstrated that such weak surface flow stabilized the downstream boundary layer significantly, leading to the complete suppression of the trailing-edge noise.

Acknowledgments

This work was partly supported by a Grant-in-Aid for Young Scientists (B) from the Japan Society for Promotion of Science (No. 24760664) and a Grant for Scientific Research from Tokyo Metropolitan Government.

References

[1] Arbey H. and Bataille J., Noise generated by airfoil profiles placed in a uniform laminar flow, *Journal of Fluid Mechanics*, Vol. 134, (1983), pp. 33-47.

[2] Corke, T.C., Enloe, C.L. and Wilkinson, S.P., Dielectric barrier discharge plasma actuators for flow control, *Annual Review of Fluid Mechanics*, Vol. 42, (2010), pp. 505-529.

[3] Desquesnes, M., Terracol M. and Sagaut P., Numerical investigation of the tone noise mechanism over laminar airfoils, *Journal of Fluid Mechanics*, Vol. 591, (2007), pp. 155-182.

[4] Inasawa, A., Asai, M. and Floryan, J.M., Certain Aspect of Instability of Flow in a Channel with Expansion/Contraction, *Proc. Seventh IUTAM Symposium on Laminar-Turbulent Transition* (*eds. Schlatter, P. and Henningson, D.S.*), Springer, (2009), pp. 501-504.

[5] Makiya, S., Inasawa, A., and Asai, M., Vortex shedding and noise radiation from a slat trailing edge, *AIAA Journal* Vol. 48, No. 2, (2010), pp. 502-509.

[6] Morkovin M.V., On roughness-induced transition: Facts, views and speculations, *Instability and Transition*, Vol. 1, (1990), pp.281-295.

[7] Nash, E.C., Lowson, M.V. and McAlpine, A., Boundary-layer instability noise on aerofoils, *Journal of Fluid Mechanics*, Vol. 382, (1999), pp. 27-61.

[8] Paterson R.W., Vogt P.G., Fink M.R. and Munch C.L., Vortex Noise of Isolated Airfoils, *Journal of Aircraft*, Vol. 10, No. 5, (1973), pp. 296-302.

[9] Post, M.L. and Corke, T.C., Separation Control on High Angle of Attack Airfoil Using Plasma Actuators, *AIAA Journal*, Vol. 42, No.11, (2004), pp.2177-2184.

[10] Reshotko, E., Disturbances in a Laminar Boundary Layer due to Distributed Surface Roughness, Turbulence and Chaotic Phenomena in Fluids; Proceedings of the International Symposium, Kyoto, Japan, 1983, pp. 39-46.

[11] Saric, W., Reed, H.L., and Kerschen, E.J., Boundary Layer Receptivity to Freestream Disturbances, *Annual Review of Fluid Mechanics*, Vol. 34, (2002), pp.291-319.

[12] Thomas, F.O., Kozlov, A. and Corke, T.C., Plasma Actuators for cylinder Flow Control and Noise Reduction, *AIAA Journal*, Vol. 46, No.8, (2008), pp.1921-1931.